

Synthesis, *In-Silico*, *In Vitro* and DFT Assessments of Substituted Imidazopyridine Derivatives as Potential Antimalarials Targeting Hemoglobin Degradation Pathway

Oberdan Oliveira Ferreira^{*}, Suraj N. Mali ^{†,§§§,****}, Bhagwat Jadhav[‡], Samir Chtita[§], Aleksey Kuznetsov[¶], Richie R. Bhandare^{||,*}, Afzal B. Shaik^{††}, Farhan Siddique^{‡‡,§§}, Akshay R. Yadav^{¶¶}, Chin-Hung Lai^{||||}, Jorddy Neves Cruz^{***}, Eloisa Helena de Aguiar Andrade^{*,†††}, Snehal Arvindekar^{‡‡‡}, Rahul D. Jawarkar^{§§§} and Mozaniel Santana de Oliveira^{†††,||||,****}

^{*}Program of Post-Graduation in Biodiversity and Biotechnology (Bionorte), Federal University of Pará, Belem 66075-110, PA, Brazil

[†]Department of Pharmaceutical Sciences and Technology, Birla Institute of Technology (Mesra Campus), Mesra 835215, Jharkhand, India

[‡]P. G. and Research Centre, Department of Chemistry, Government of Maharashtra, Ismail Yusuf College of Arts, Science and Commerce, Mumbai, India

[§]Laboratory of Analytical and Molecular Chemistry of Sciences Ben M'Sik, Hassan II University of Casablanca, B. P. 7955 Sidi Othmane, Casablanca, Morocco

[¶]Department of Chemistry, Universidad Técnica Federico Santa Maria, Avenida Santa Maria 6400, Vitacura 7660251, Santiago, Chile

^{||}Department of Pharmaceutical Sciences, College of Pharmacy and Health Science, Ajman University, Ajman P. O. Box 346, UAE

^{**}Center of Medical and Bio-Allied Health Sciences Research, Ajman University, Ajman, UAE

^{††}St. Mary's College of Pharmacy, St. Mary's Group of Institutions Guntur, Affiliated to Jawaharlal Nehru Technological University Kakinada, Chebrolu, Guntur 522212, Andhra Pradesh, India

^{‡‡}Laboratory of Organic Electronics, Department of Science and Technology, Linköping University, SE-60174 Norrköping, Sweden

^{§§}Department of Pharmaceutical Chemistry, Faculty of Pharmacy, Bahauddin Zakariya University 60800, Multan, Pakistan

^{¶¶}Department of Pharmaceutical Chemistry, KES'S, Rajarambapu College of Pharmacy, Kasegaon 415404, Maharashtra, India

^{||||}Department of Medical Applied Chemistry, Chung Shan Medical University, Taichung 40241, Taiwan

^{***}Laboratory of Functional and Structural Biology, Institute of Biological Sciences, Universidade Federal do Pará, Belem 66075-110, Brazil

^{†††}Adolpho Ducke Laboratory, Coordination of Botany, Emilio Goeldi Museum of Pará, Belem 66077-830, Brazil

^{‡‡‡}Department of Pharmaceutical Chemistry, Bharati Vidyapeeth College of Pharmacy, Kolhapur, Maharashtra, India

^{§§§}Department of Medicinal Chemistry and Drug Discovery, Dr. Rajendra Gode Institute of Pharmacy, University Mardi Road, Amravati 444603, India

^{****}mali.suraj1695@gmail.com

|||||mozaniel.oliveira@yahoo.com.br

^{****}Corresponding authors. E-mails: mali.suraj1695@gmail.com; mozaniel.oliveira@yahoo.com.br

Received: 31 May 2023

Accepted: 4 July 2023

Published: 26 July 2023

ABSTRACT: Malaria is a serious illness transmitted through the bite of an infected mosquito, which is caused by a type of parasite called plasmodium and can be fatal if left untreated. Thus, newer antimalarials with unique mode of actions are encouraged. Fused pyridines have been vastly reported for numerous pharmacological activities including but not limited to analgesics, antitubercular, antifungal, antibacterial and antiapoptotic agents. In a current study, a series of substituted Imidazo[1,2-a]pyridine-3-carboxamides (IMPCs) (SM-IMP-01-13) along with some hydrazides (DA-01-DA-02) were synthesized and characterized by Fourier-transform infrared spectroscopy (FTIR), $^1\text{H}/^{13}\text{C}$ -NMR (proton/carbon nuclear magnetic resonance), elemental analyses and mass spectra. These synthesized analogies were subjected for *in vitro* biological activities such as Brine Shrimp lethality (BSL), and assay of β -hematin formation inhibitions. The BSL assay results suggested that compounds, SM-IMP-09, SM-IMP-05 were found to be less toxic and they also had comparable toxicity as of 5-Fluorouracil (control) (e.g., at 10 $\mu\text{g}/\text{ml}$: 20% deaths of nauplii). Derivatives SM-IMP-02, and DA-05 inhibited β -hematin formation: IC_{50} : 1.849 and 0.042 μM , respectively). Our molecular docking analysis on plasmodial cysteine protease falcipain-2 indicated that compound DA-05 (−9.993 kcal/mol) had highest docking score and it was comparable to standard Chloroquine (−7.673 kcal/mol). The most active molecule, DA-05 was also retained with lower HOMO–LUMO energy gap as 3.36 eV. Further, we have also analyzed MEP, and other global reactivity indexes for all IMPCs using DFT. Finally, our *in-silico* pharmacokinetic analysis suggested that all compounds were having good% human oral absorption values ($\approx 100\%$), good Caco-2 cell permeabilities (>1600 nm/s), and non-carcinogenic profiles.

KEYWORDS: Pyrimidine; heterocycles; docking; *Plasmodium falciparum*; antimalarial activity.

1. INTRODUCTION

Malaria is a severe infectious illness that impacts millions of individuals globally every year.¹ The most lethal parasite responsible for malaria is *Plasmodium falciparum*, causing the majority of malaria-related fatalities.² The disease spreads through mosquito bites, and also has the complicated life cycle of the parasite, as well as its resistance to insecticides and drugs, contribute to the proliferation of the disease.³ *P. falciparum* is becoming more resistant to available drugs, such as antifolates and chloroquine, due to random mutations.⁴ Although five *Plasmodium* parasite species can cause malaria in humans, *P. falciparum* and *P. vivax* cause the majority of malaria-related deaths. Artemisinin-based Combination Therapies (ACTs) are the present standard treatment for *P. falciparum* malaria.⁴ Despite advancements in drug development, preventing and controlling malaria remains difficult due to the widespread emergence of drug-resistant *P. falciparum* strains. This has limited the efficacy of current drug treatments, including ACTs. To combat drug-resistant *P. falciparum* malaria, new drug molecules and alternative therapies are needed.⁴ Artemisinin (ART) is a natural antimalarial compound that effectively treats *P. falciparum* malaria. It functions by creating highly reactive free radicals and reactive oxygen species when interacting with iron. Targeting β -hematin formation is a crucial target in hemozoin formation pathway of *Plasmodium spp.*⁵ Inhibitors of β -hematin

formation result in immediate protozoal deaths. Thus, development or repurposing of new antimalarial hits against the ‘Haemoglobin degradation’ (HD) pathway which is considered as a very crucial target in antimalarial drug discovery process.⁵ The HD pathways are basically a catabolic process that is required for the intraerythrocytic development of malaria parasites.

Fused imidazopyridines share a structural resemblance to the purines, which thus enables to have their biological investigations in order to find out potential lead/hit candidates of therapeutic values.^{6–8} The discovery of first GABA_A receptor agonist divulged their medicinal chemistry potentials.^{9,10} Numerous enzyme inhibitors such as aromatase inhibitors, classical non-steroidal anti-inflammatory agents and proton pump inhibitors have imidazopyridine (IMP) core in them.⁷ They have been widely reported for varieties of pharmacological actions including but not limited to Antitumor activity, antimicrobial activity, anti-inflammatory activity, antiviral activities, anxiolytic, antiprotozoal, in the treatment of immune-related diseases, Antidiabetic activity, angiotensin II receptor antagonists and antitubercular agents.^{7–24} Furthermore, many marketed drug candidatures bear IMP moiety in their cores such as olprinone (acute heart failure), zolpidem (insomnia), alpidem (anxiolytic), necopidem and saripidem (anti-anxiolytic), zolimidine (peptic ulcer) and rifaximin (antibiotic) (Fig. 1).⁷ Recently, we have summarized biological potential of IMPs against

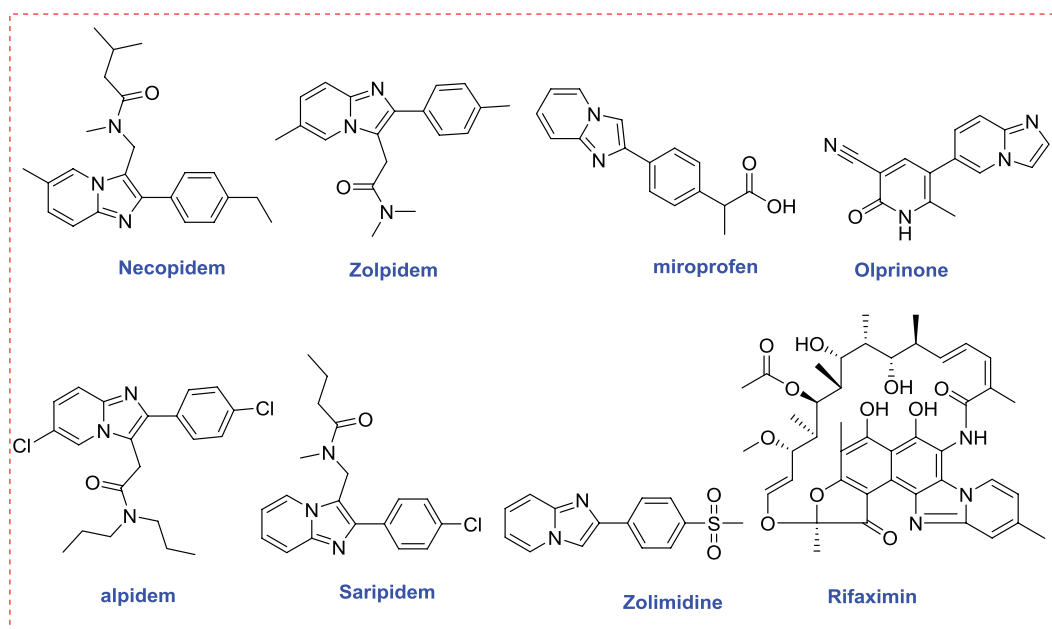


Fig. 1. (Color online) Structures of some marketed IMP analogues.

diseases of neglected populations such as malaria, trypanosomiasis and tuberculosis (TB).^{10–16}

Hydrazide-hydrazone are very well-known for their potent biological activities such as anti-TB and antibacterial or antiviral activities.^{25–29} To our best knowledge, only a handful of literature reports on the synthesis of IMP-hydrazone are available.^{13,30} However, in year 2021 a group of scientists from ‘Shiraz University of Medical Sciences, Shiraz, Iran’ successfully prepared a series of 12 imidazo[1,2- α]pyridine derivatives bearing 1,2,3-triazole moiety containing hydrazone in reporting their antiproliferative potential against lung and pancreatic cancer cells as *c*-Met kinase inhibitors.³⁰ Previously, Kumar *et al.*,¹ demonstrated the antimalarial activity of newer acyl hydrazone compounds and docked against the target plasmidial ‘cysteine protease falcipain-2 (FP-2)’. Figure 2 displays known antimalarial agents.

With similar analogy but with different synthetic approaches, we aimed to synthesize IMP carbohydrazone derivatives (DA-01 to DA-05). We have also carried out synthesis of previously reported substituted 2,7-dimethylimidazo[1,2-*a*]pyridine-3-carboxamides derivatives (SM-IMP-01 to SM-IMP-13) and repurposed for checking different biological potentials other than anti-TB activity.¹⁰ Such hybridized structures (DA-01 to DA-05) including (SM-IMP-01 to SM-IMP-13), in total 18 compounds, were subjected for *in vitro* antimalarial, and Brine Shrimp lethality (BSL) assessments (*Supporting information*,

Tables S1–S5, Figs. S1–S6). All synthesized compounds were thoroughly characterized for ¹H-NMR, ¹³C-NMR, FTIR, mass, and for elemental analysis (*Supporting information*, Figs. S7–S66). Molecular hybridization has emerged as a powerful tool where molecules containing more than one structural units are synthesized with improved biological activity than their corresponding lead compound. Its aim is to identify novel, highly active compounds by combining two principles with observed synergistic pharmacological activities. In particular, we coupled imidazopyridines to hydrazone core to have imidazopyridine-based hydrazone analogues.

In this particular study, the goal was to develop effective antimalarial agents against *P. falciparum*. To do so, we tested 18 previously reported substituted imidazo[1,2-*a*]pyridine-3-carboxamides (IMPCs) (SM-IMP-01–013) along with some hydrazides (DA-01–DA-05) (Scheme 1). Herein, there are three imidazopyridine carboxamide (IMPC) series, (1) with 6,8-dibromo-, (2) with 6-bromo only (at eighth position H) and (3) hydrazides of 6-bromo series. These 18 derivatives were then analyzed using molecular modeling techniques,^{31–33} including protein-ligand docking against *P. falciparum* cysteine protease FP-2 (PDB ID: 3BPF) using the flexible docking method and the simulation-based docking protocol with Glide module of Schrodinger, LLC, NY, 2022 drug discovery suite. We also assessed absorption, distribution, metabolism, excretion, and toxicity (ADMET) properties.

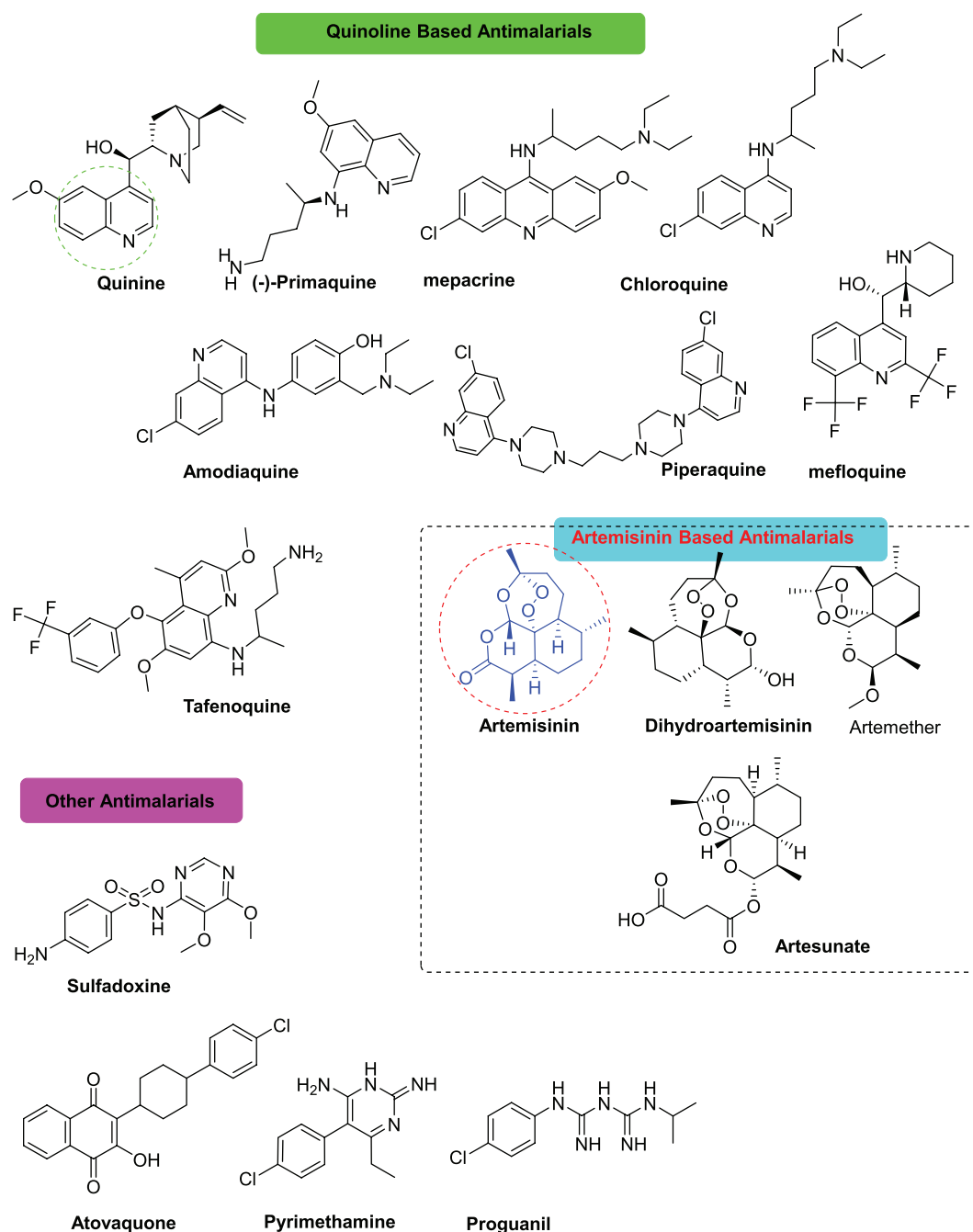


Fig. 2. (Color online) Classification of malarial drugs based on the scaffold and their structures. Adapted with permission from Ref. 50. Copyright 2019 Elsevier.

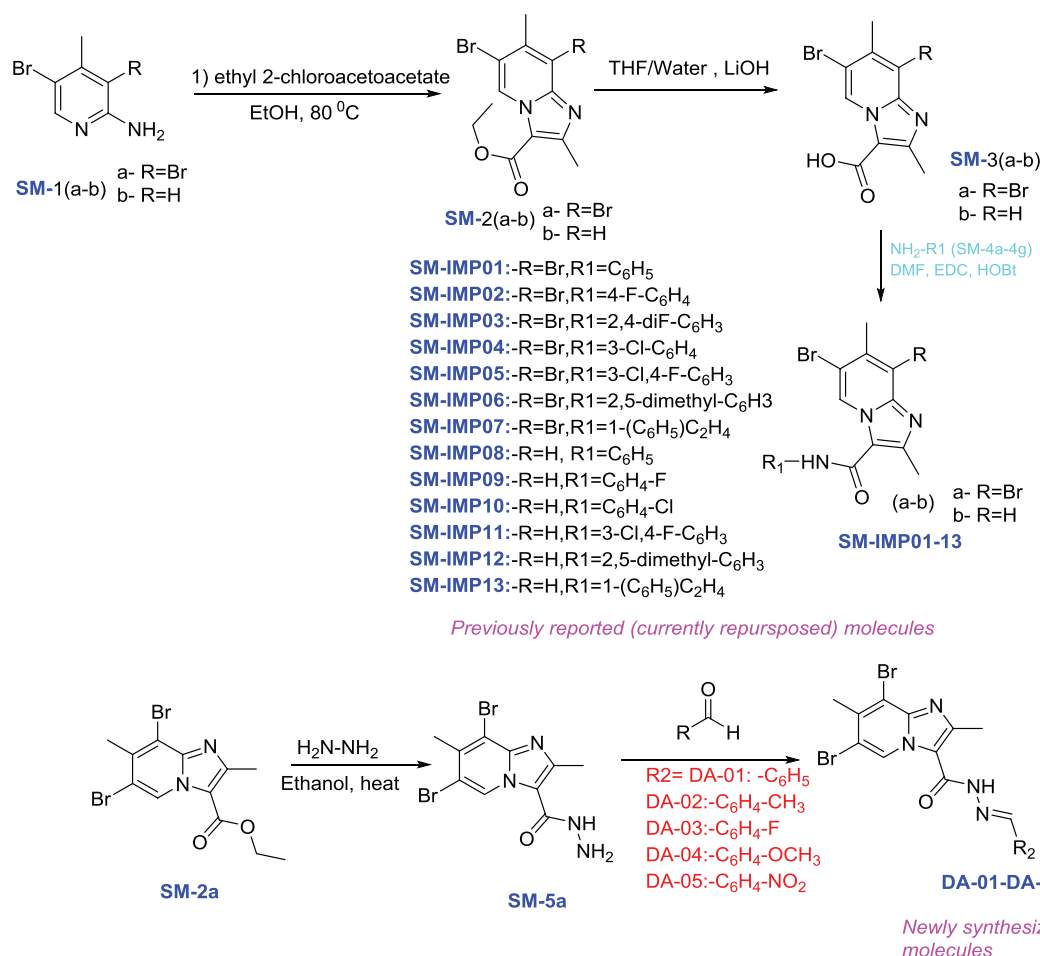
To confirm the antimalarial potential of the best docked compounds, we calculated the MM-GBSA-based free binding energies of docked complexes against the *P. falciparum* FP-2 enzyme. Furthermore, we also evaluated cytotoxicity analysis using BSL bioassay. Finally, theoretical analysis was performed by calculating DFT properties^{34–38} and compared with observed bioactivities. In addition to this, we conducted extended antimicrobial, and anti-inflammatory

activities and are attached in *supporting information*.^{39–49}

2. RESULTS AND DISCUSSION

2.1. Synthesis

Synthesis of all 18 compounds were carried out as per the previously reported protocols^{10,13} and as described



Scheme 1. Reaction scheme for preparation of compounds (SM-IMP-01) to (SM-IMP-13) and (DA-01-05)^{10,13} (reproduced from Refs. 10 and 13).

in the section ‘Chemistry’ of ‘3. Materials and methods’ (Scheme 1).

2.2. Bioactivity analysis

For a set of 18 imidazopyridines, we have conducted two assays: (1) BSL assay and (2) inhibition of β -hematin formation Assay. The BSL assay is an bioassay used to evaluate cytotoxicity of synthesized compounds or natural compounds. The basic principle behind this assay is based on the killing ability of tested compounds on brine shrimp (*Artemia salina*, a simple organism). Thus, in order to have better assessments of our IMPs, we first checked their cytotoxicities followed by β -hematin formation Assay.

2.2.1. Brine shrimp lethality assay (BSL assay)

For current set of imidazopyridine analogues, we estimated preliminary cytotoxicity (estimation of killing

of a laboratory cultured larvae (nauplii) using the ‘Brine shrimp (*Artemia salina*) lethality assay’ (for procedure, please refer supporting information).^{39–41} The BSL assay for all 18 compounds demonstrated that some of compounds had higher cytotoxicity (e.g., at 1 $\mu\text{g/ml}$: SM-IMP-03, SM-IMP-07, SM-IMP-13, DA-01: >40% deaths of nauplii); while some of compounds (e.g., at 1 $\mu\text{g/ml}$: SM-IMP-02 (10% death of nauplii), SM-IMP-09 (10% death of nauplii), SM-IMP-05 (10% death of nauplii) were found to be less toxic and they also had comparable toxicity as of 5-Flurouracil (control) ((e.g., at 10 $\mu\text{g/ml}$: 20% deaths of nauplii). We used distilled water (DW) as a negative control, wherein vincristine sulphate was used as positive control. We also, used 5-FU as a positive control. With DW, no mortalities were observed, while in case of vincristine sulphate control, we noticed 94% deaths of nauplii at 1 $\mu\text{g/ml}$. Results for BSL assay are represented in Fig. 3 and Table S1 (Supplementary Material).

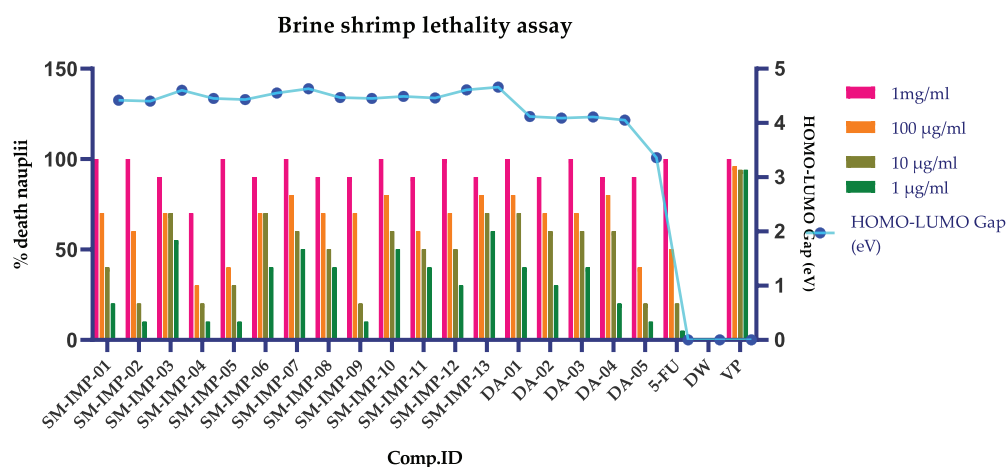


Fig. 3. (Color online) The results of BSL assay of tested compounds as (SM-IMP-01) to SM-IMP-13), and (DA-01-05), respectively. Wherein, DW was used as negative control, wherein 5-Fluorouracil was used a positive control.

2.1.2. *In vitro* inhibition of β -Hematin formation Assay

Results from *in vitro* antimalarial activity, i.e., β -hematin formation assay for a set of 18 compounds (SM-IMP-01) to (SM-IMP-13) and (DA-01-05) are presented in Table S3 (Supplementary Material).^{48,49} The β -hematin formation inhibitions were expressed in percentage (*I*%) and results were obtained by triplicate repetitions ($n = 3$). It can be seen that for the first series containing 6,8-dibromo substituents, molecule SM-IMP-02 was found with IC_{50} value of $1.849 \mu M$; when tested with *in vitro* inhibition of β -hematin formation assay. For second series with only 6-bromo substitution, molecule SM-IMP-09 retained IC_{50} value of $2.486 \mu M$. For the third series, which was having hydrazide core in it, molecule DA-05 was found with lowest IC_{50} value. Among all three series of compounds, SM-IMP-13 was found to be least active for inhibition of β -hematin formation, compared to the standard anti-malarial drug, Chloroquine ($IC_{50} = 0.054 \mu M$, Reported: $IC_{50} = 0.04 \pm 0.002 \mu M$, $IC_{90} = 0.35 \pm 0.006 \mu M$).⁴⁸

2.3. Molecular docking

2.3.1. Targeting hemoglobin degradation pathway (*Plasmodium falciparum* Cysteine protease falcipain-2 (protein))

The *Plasmodium falciparum* has a very complex life cycle and has a number of biological targets, which can be used to discover newer antimalarial agents. Among

various targets, hemoglobin degradation pathway would have also been targeted for effective treatment of malaria.¹ Prior literature data¹ suggest that ‘the falcipain family proteases’ (FP-2 and FP-3) are crucial targets in the hemoglobin hydrolysis. Thus, by inhibiting these targets one can avoid hemoglobin hydrolysis and thus, retard the parasitic growth. It is important to note that ‘non-peptide based’ inhibitors would offer added advantages than peptide and peptidomimetic inhibitors with less metabolic degradations and absorption profiles than later.¹ The selection of protein database id (3bpf) was based on previous available data on imidazopyridines or hydrazones as antimalarials.^{1,14} Previous *in-silico* analysis on imidazopyridines suggested that this scaffold had better binding scores than standard like Chloroquine (docking score: -7.673 kcal/mol).^{1,14} Docking analysis showed that the catalytical triad **Gly83**, **Cys42** and **His174** residues were retained for our best docked molecules (SM-IMP-02) and (DA-05) with docking scores of -9.783 kcal/mol and -9.993 kcal/mol, respectively. Further detailed analysis of scores and binding sites residues (Figs. 4–7) have been given in Table 1 (Supporting information, Table S6). The lowest IC_{50} value of DA-05 is well comparable to higher binding free energy scores on pdb id:3BPF as -55.91 Kcal.mol⁻¹.

2.3.2. Validation of docking protocols

We validated the docking protocol used herein by re-docking of native co-crystallized ligand, E64 (N-[N-(L-3-trans-carboxyirane-2-carbonyl)-L-leucyl]-agmatine) within same binding site (the catalytical

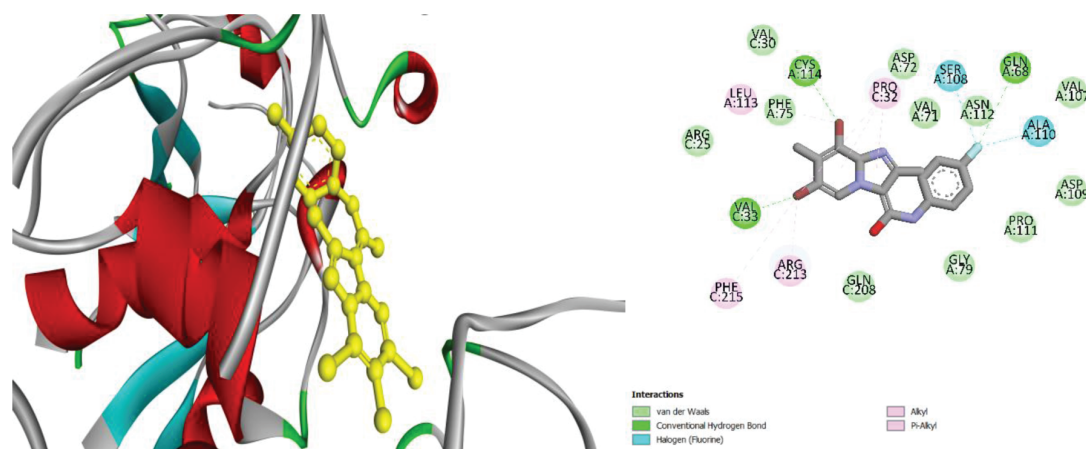


Fig. 4. (Color online) 3D- and 2D-binding pocket of best docked molecule (among first and second series), SM-IMP-02 within the protein PDB ID: 3bpf.

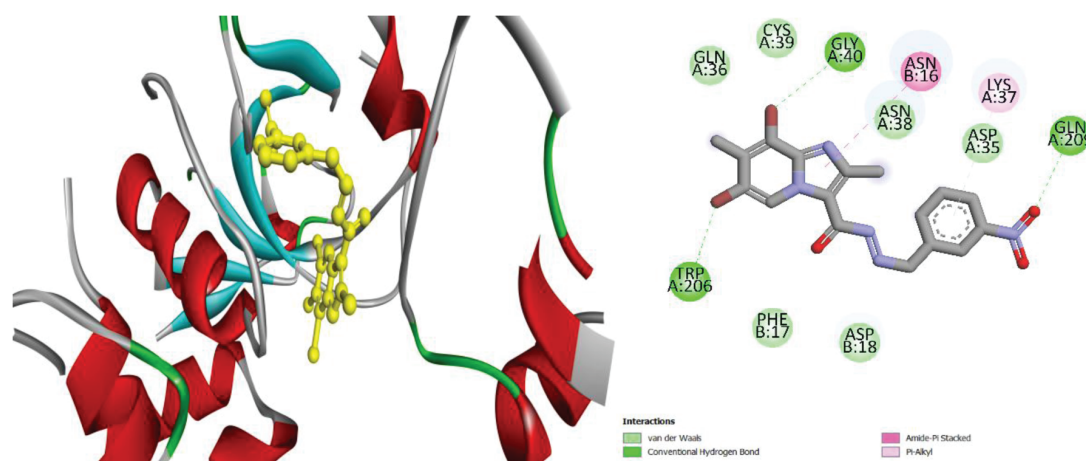


Fig. 5. (Color online) 3D- and 2D-binding pocket of best docked molecule (among all three series), DA-05 within the protein PDB ID: 3bpf.

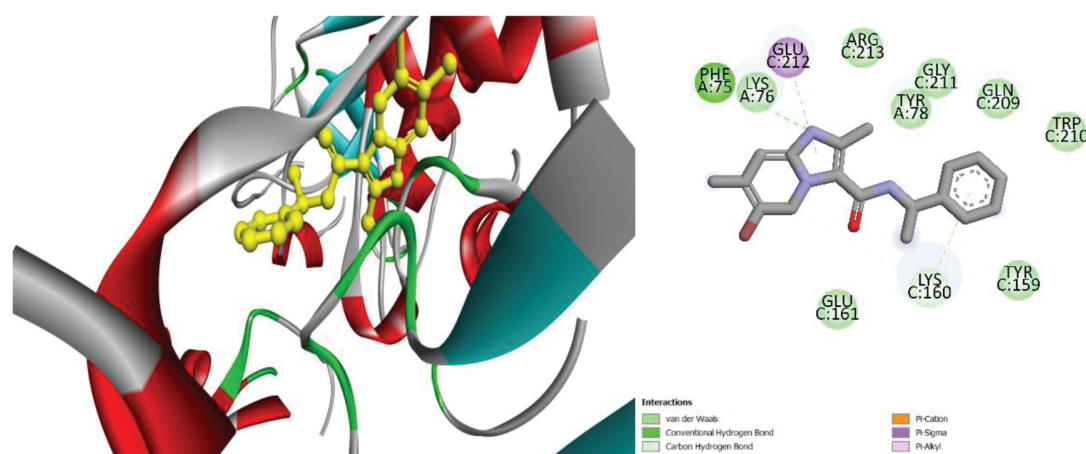


Fig. 6. (Color online) 3D- and 2D-binding pocket of least docked molecule (among all three series), SM-IMP-13 within the protein PDB ID: 3bpf.

triad Gly83, Cys42 and His174).¹ We retained RMSD values less than 2 Å, suggesting that docking protocols used were validated successfully (Table S7, please refer supporting information).¹⁴

Table 1. The docking scores (kcal/mol) of all 18 IMPs against a corresponding target (PDB ID: 3bpf).

| Comp.ID/Std. | 3BPF |
|--------------------|---|
| | <i>Plasmodium falciparum</i> |
| SM-IMP-01 | -8.187 |
| SM-IMP-02 | -9.783 (Among first and second series) |
| SM-IMP-03 | -9.291 |
| SM-IMP-04 | -8.30 |
| SM-IMP-05 | -6.761 |
| SM-IMP-06 | -7.477 |
| SM-IMP-07 | -9.344 |
| SM-IMP-08 | -7.331 |
| SM-IMP-09 | -7.445 |
| SM-IMP-10 | -7.562 |
| SM-IMP-11 | -7.689 |
| SM-IMP-12 | -3.210 |
| SM-IMP-13 | -3.183 |
| DA-01 | -9.359 |
| DA-02 | -9.696 |
| DA-03 | -8.341 |
| DA-04 | -8.593 |
| DA-05 | -9.993 (Best docked: For series third) |
| Chloroquine (Std.) | -7.673 |

2.4. Prime-(MM/GBSA) calculations

The Prime-MM/GBSA (Molecular mechanics with generalized Born and surface area solvation) is one of the important methods in computer-aided drug designing to calculate binding energies of selected ligand or set of ligands against target chosen. From our MM/GBSA calculations, it was clear that the best docked molecules from set of SM-IMP-01 to SM-IMP-13 and DA-01 to DA-05 represented higher (more stable) energies [for 3BPF: DA-05: MMGBSA dgBind energy: $-55.91 \text{ KJ.mol}^{-1}$] compared with standard drug, Chloroquine (against 3BPF: MMGBSA dgBind energy: $-42.96 \text{ KJ.mol}^{-1}$).

2.5. Theoretical analyses

Optimization energies, dipole moment, polarizability, and HOMO to LUMO (highest occupied molecular orbital and the lowest unoccupied molecular orbital, respectively) gap values are represented in Table 2.^{34–38,51} These structures of compounds have the lowest energy minima and lowest energy conformers. Various molecular properties are calculated by using the HOMO–LUMO energy gap of the investigated compounds (SM-IMP-01–SM-IMP-13) and (DA-01 and DA-05) such as optical and electronic properties and molecular stability and reactivity.^{37,38} Figure 8 shows all the structures that have been optimized. Low values of energy gap and LUMO lead to increased biological activity.^{14,37,38} This is due to the low energy required for electronic excitation and the strong charge transfer interaction between donor and acceptor atoms. The optimization of the HOMO–LUMO

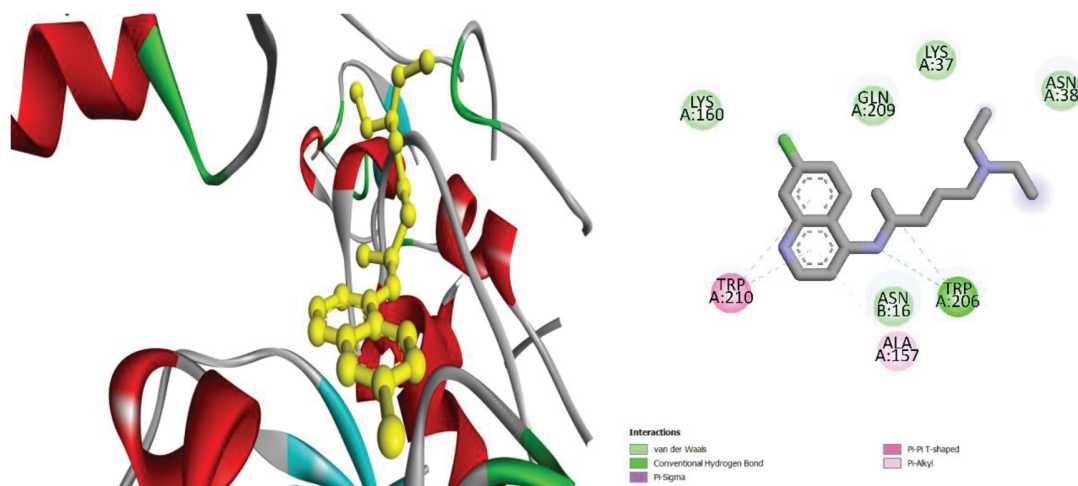
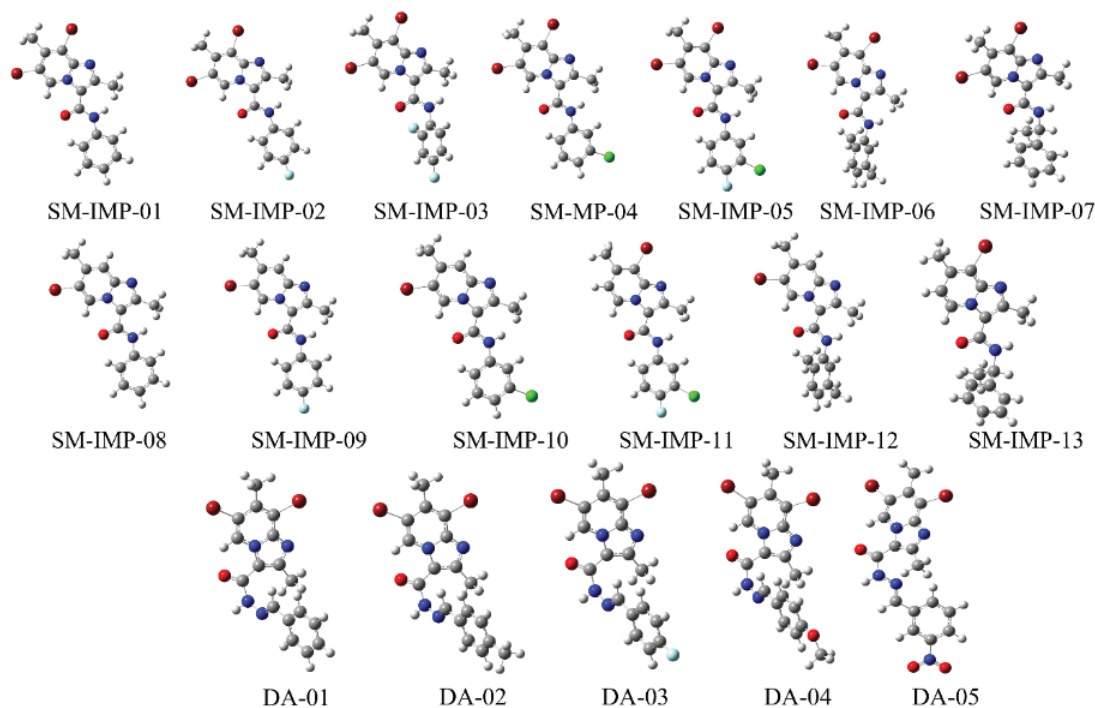


Fig. 7. (Color online) 3D- and 2D-binding pocket of standard drug Chloroquine within the protein PDB ID: 3bpf.

Table 2. Optimization energies, HOMO and LUMO energies and their gap calculated in gas phase at B3LYP/6-311+G(d, p) level of DFT calculations.

| Structure code | Optimization energy (a.u.) | Dipole moment (debye) | Polarizability (α) (a.u.) | E_H (eV) | E_L (eV) | E_g (eV) |
|----------------|----------------------------|-----------------------|------------------------------------|------------|------------|------------|
| SM-IMP-01 | -6005.59 | 1.54 | 279.71 | -6.22 | -1.81 | 4.42 |
| SM-IMP-02 | -6104.85 | 1.92 | 279.47 | -6.27 | -1.87 | 4.40 |
| SM-IMP-03 | -6204.12 | 2.51 | 272.55 | -6.42 | -1.82 | 4.60 |
| SM-IMP-04 | -6465.21 | 0.89 | 295.07 | -6.38 | -1.93 | 4.45 |
| SM-IMP-05 | -6564.47 | 2.42 | 295.21 | -6.41 | -1.98 | 4.43 |
| SM-IMP-06 | -6084.25 | 1.97 | 299.94 | -6.27 | -1.72 | 4.55 |
| SM-IMP-07 | -6084.24 | 2.18 | 289.36 | -6.29 | -1.66 | 4.63 |
| SM-IMP-08 | -3432.05 | 2.01 | 257.27 | -6.10 | -1.64 | 4.47 |
| SM-IMP-09 | -3531.32 | 3.27 | 256.95 | -6.16 | -1.71 | 4.45 |
| SM-IMP-10 | -3891.67 | 2.23 | 272.48 | -6.26 | -1.78 | 4.49 |
| SM-IMP-11 | -3990.93 | 3.14 | 272.02 | -6.26 | -1.80 | 4.46 |
| SM-IMP-12 | -3510.71 | 1.88 | 277.48 | -6.15 | -1.54 | 4.61 |
| SM-IMP-13 | -3510.70 | 1.68 | 267.21 | -6.11 | -1.45 | 4.66 |
| DA-01 | -6099.03 | 2.18 | 300.72 | -6.33 | -2.22 | 4.12 |
| DA-02 | -6138.36 | 3.09 | 316.75 | -6.22 | -2.13 | 4.09 |
| DA-03 | -6198.29 | 1.17 | 300.85 | -6.39 | -2.29 | 4.11 |
| DA-04 | -6213.59 | 4.24 | 322.05 | -6.06 | -2.02 | 4.05 |
| DA-05 | -6303.60 | 2.74 | 330.88 | -6.51 | -3.14 | 3.36 |

**Fig. 8.** (Color online) Optimized structures of the investigated compounds at B3LYP/6-311+G(d, p) level of DFT calculations in the gas phase.

energy gap and other descriptors is crucial for understanding the chemical reactivity of new inhibitors and their structure. This information can be very insightful.^{14,37,38} A larger energy gap corresponds to greater kinetic stability and lower polarizability, resulting in lower reactivity. Conversely, a smaller energy gap indicates lower stability, increased polarizability and greater chemical reactivity (Table 3).¹⁴ Among the 6,8-dibromo-IMP series, i.e., (SM-IMP-01-SM-IMP-07), compound **SM-IMP-07** (4.63 eV) has larger energy gap; wherein **SM-IMP-02** (4.40 eV) had lower energy gap. Further moving to next series of IMPs, with only 6-bromo substitution (Hydrogen at eighth position), i.e., (SM-IMP-08-SM-IMP-13), compound **SM-IMP-13** (4.66 eV) represented higher energy gap (Fig. 9). Thus, with reference to previously known analogy, compounds with lower energy gaps tend to more reactive than compounds with larger energy gaps. Similarly, for third series of hydrazides compounds, DA-1-DA-05 (in range of 3.12–4.12 eV) are with the small energy gaps and more reactive as compared to the SM-IMP-01-13 serials. Supporting Figs. S70 and S71 show the HOMO–LUMO orbital with energy gap values and labels.

Table 3. Global reactivity descriptors of the targeted compounds.

| Structure code | μ (eV) | χ (eV) | η (eV) | S (eV) | ω (eV) |
|----------------|------------|-------------|-------------|--------|---------------|
| SM-IMP-01 | -4.01 | 4.01 | 1.31 | 0.65 | 10.52 |
| SM-IMP-02 | -4.07 | 4.07 | 1.26 | 0.63 | 10.48 |
| SM-IMP-03 | -4.12 | 4.12 | 1.39 | 0.70 | 11.83 |
| SM-IMP-04 | -4.15 | 4.15 | 1.26 | 0.63 | 10.85 |
| SM-IMP-05 | -4.19 | 4.19 | 1.23 | 0.61 | 10.77 |
| SM-IMP-06 | -4.00 | 4.00 | 1.42 | 0.71 | 11.30 |
| SM-IMP-07 | -3.98 | 3.98 | 1.49 | 0.74 | 11.76 |
| SM-IMP-08 | -3.87 | 3.87 | 1.41 | 0.71 | 10.59 |
| SM-IMP-09 | -3.93 | 3.93 | 1.37 | 0.69 | 10.61 |
| SM-IMP-10 | -4.02 | 4.02 | 1.36 | 0.68 | 10.95 |
| SM-IMP-11 | -4.03 | 4.03 | 1.33 | 0.66 | 10.81 |
| SM-IMP-12 | -3.85 | 3.85 | 1.54 | 0.77 | 11.37 |
| SM-IMP-13 | -3.78 | 3.78 | 1.60 | 0.80 | 11.45 |
| DA-01 | -4.27 | 4.27 | 0.95 | 0.47 | 8.68 |
| DA-02 | -4.17 | 4.17 | 0.98 | 0.49 | 8.52 |
| DA-03 | -4.34 | 4.34 | 0.91 | 0.45 | 8.56 |
| DA-04 | -4.04 | 4.04 | 1.02 | 0.51 | 8.28 |
| DA-05 | -4.83 | 4.83 | 0.11 | 0.60 | 1.29 |

When the chemical potential (μ) falls, it becomes harder to lose an electron but simpler to gain one. It measures the escape propensity of electrons and is connected to molecular electronegativity. Compound DA-05 is the least stable and most reactive of all the examined series, as seen in Table 3. The ability of a molecule to draw electrons is called electronegativity (χ). Compounds DA-05 and SM-IMP-05 exhibit higher electronegativity values than the other compounds, according to the (χ) values in Table 3. Concepts like hardness (H) and softness (S) can aid in your comprehension of how chemical systems behave. A soft molecule has a low energy gap compared to a hard molecule's wide energy gap. From theoretical calculations established, it was found that the molecule **SM-IMP-05** retained less value of chemical hardness (within 6,8-dibromo series); wherein **SM-IMP-11** had low hardness value among 6-bromo series. Overall, among series 1 and 2 (6,8-dibromo and 6-bromo), compound **SM-IMP-05** had less value of chemical hardness (1.23 eV). For the third series, hydrazides, we found that compound **DA-05** (0.11 eV) had less value of chemical hardness. In terms of softness, the molecules, **SM-IMP-13** and **DA-05** had the highest softness ($S = 0.80$ eV, and 0.60 eV, respectively). Electrophilicity (ω) is a measure of the energy of stabilization experienced by a system when it is saturated with electrons from the surrounding environment.^{14,37,38} This reactivity parameter serves as an indicator of a molecule's ability to

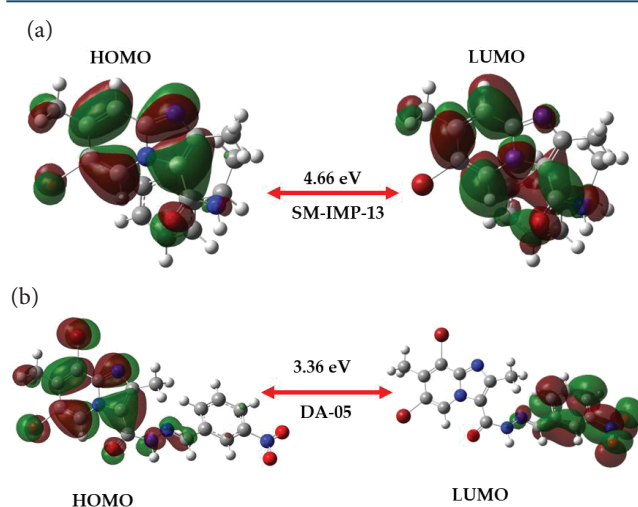


Fig. 9. (Color online) The contour plots of HOMOs and LUMOs for the SM-IMP-13 (one with highest HOMO–LUMO energy gap) and DA-05 (one with lower HOMO–LUMO energy gap) compounds (the isovalue = 0.02 a.u.).

donate or accept charge. A lower value of ω indicates the presence of a highly reactive nucleophile, while higher values suggest the presence of a strong electrophile.¹³ Our results revealed that, hydrazide molecule **DA-05** (1.29 eV) had lower value of (ω), thus, compound can be considered as a good nucleophile. However, molecule SM-IMP-03 is a good electrophile.

2.5.1. Molecular electrostatic potential (MEP)

In biochemistry and pharmacology, molecular electrostatic potentials (MEPs) have been widely employed to find distinctive patterns of positive and negative potentials that either promote or inhibit specific types of biological processes.¹³ It is generally known that the reactive behavior of a molecule can be understood and predicted using the electrostatic potential estimated over a molecular surface. The **electrostatic potential** maps were generated to determine the charge distribution around a **molecule** and therefore determine the regions that could form hydrogen bonding.¹³ MEP investigations are utilized to locate electrophilic and nucleophilic areas in designed compounds, which can help predict reactive sites. Figure S72 illustrates this process, where negative, positive and neutral zones on MEP surfaces are depicted in red, blue and green colors, respectively. The oxygen atom is surrounded by a mostly negative, red zone, which is somewhat hindered by the presence of surrounding carbons and the attachment of bromine. Structure showing negative

regions are in good correlation for attachment and attracting the potential electrophiles as in the SM-IMP-05, SM-IMP-07 and DA-05, respectively. Figure 10 shows the MEP plots for best bioactive molecules, SM-IMP-02, SM-IMP-09 and DA-05. Whereas, we also depicted the MEP plot for least bioactive molecule, SM-IMP-13.

2.5.2. Mulliken charge distribution analysis

These calculations have important aspects in the application of quantum chemical calculation to molecular system because of atomic charges effecting dipole moment, electronic structure, molecular polarizability and a lot more properties of molecular systems. The analysis of the frontier orbitals for the title chemicals showed that all the orbital transitions from HOMO to LUMO involve the $\pi\pi^*$ transition mixing with some degree of the $n\pi^*$ transition except for **DA-05**. For **DA-05**, such orbital transition involves a charge transfer. The difference in the orbital transitions might indicate that there was neither an electron-donating nor an electron-accepting region in the studied compounds besides **DA-05**. Therefore, the atomic Mulliken charges of the studied compounds were taken to investigate the charge distribution of the title compounds in this study. As depicted in Supplementary Fig. S73, the oxygen atom on the carbonyl group bears the most negative charge compared with the other atoms among all the studied compounds.

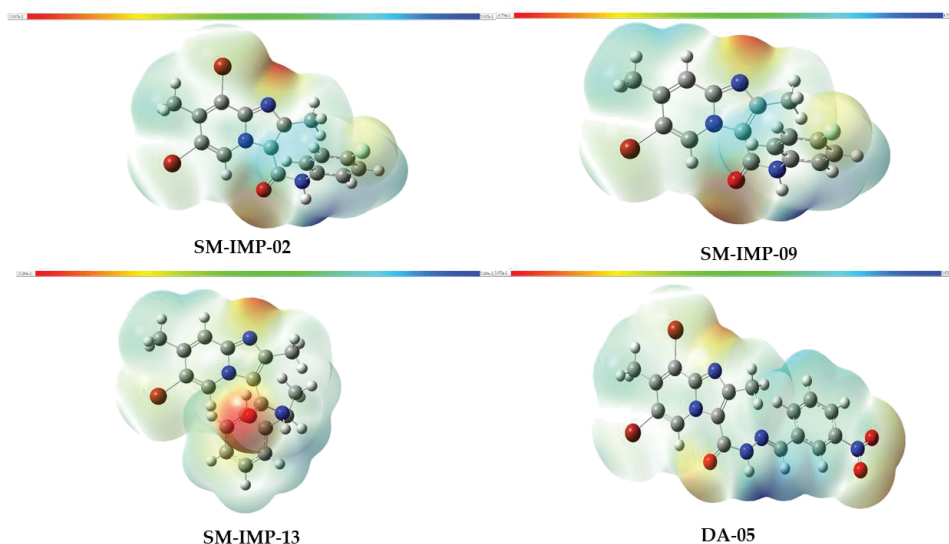


Fig. 10. (Color online) MEP maps for the investigated compounds (SM-IMP-02 (best active in 6,8-dibromo series), SM-IMP-09 (best active in 6-bromo series), DA-05 (best active in hydrazide series) and SM-IMP-13 (least bioactive among all three series).

2.6. Antimalarial activity of the Substituted Imidazopyridines (IMPs) (SM-IMP-01 to SM-IMP-13, and DA-01-05) and calculated Density-functional theory (DFT)-based theoretical properties

In order to check the potential antimalarial activities of the said 18 IMPs, we subjected them against β -hematin formation assay (Fig. 11). The *in vitro* analysis results indicate that the presence of a halogen, specifically (-Br) at the sixth and eighth positions of the bromo-IMPCs (series first, second and third) (as shown in Scheme 1), strongly influences the outcome. In the first series (SM-IMP-01 to SM-IMP-07), it was observed that the IC_{50} value for SM-IMP-02 (IC_{50} (μM): 1.849) was lower compared to the 6,8-dibromo series. This may be attributed to the presence of a 4-F substituent at the terminal phenyl ring of the hydrazide core. Comparing SM-IMP-02 with other molecules, SM-IMP-04 and SM-IMP-05, we found that IC_{50} values were slightly increased. With the exception of molecule SM-IMP-01, other compounds with 2,5-dimethyl (SM-IMP-06) and ethyl functionalities (SM-IMP-07) tend to lower the bioactivity. Moving on to another series featuring 6-bromo-IMPCs (with only one -Br on the IMP scaffold, located at the sixth position), it was observed that the absence of the -Br group at the eighth position had a significant impact, as evidenced by the higher IC_{50} values for inhibition of β -hematin formation with the same aldehyde substituents. This

also indicates the fact that if we compare two series (first and second), compounds with 6,8-dibromo substituents are more potent antimalarials than those with 6-bromo substitution. In addition, electron releasing substituents attached on the terminal aryl (-Ar) would likely increase the bioactivity. Among hydrazide series (third series) (DA-01-DA-05), compounds with -NO₂ substituent, i.e., DA-05 demonstrated strong activity. Further, we noticed that except -NO₂ substituent on aryl moiety attached to (IMP-C = O-NH---) functionality would be giving better results compared to other substituents of electron-releasing or electron-withdrawing natures. This also points out the fact that hydrazide core has substantially increased the bioactivity of -bromo series (second series).

The *in vitro* bioactivity trend among all three series was also seen when we compare their associated HOMO-LUMO energy gaps.¹³ In the final series, which comprised five hydrazides of IMPCs, it was found that they displayed lower HOMO-LUMO energy gaps, leading to higher antimalarial activities. The smaller energy gaps observed in the hydrazides (DA-01-DA-05) can be explained by their electronic properties, which may influence their bioactivities either positively or negatively.¹³ Among the 18 compounds evaluated in our β -hematin formation assays, DA-05 (with a smaller energy gap of 3.36 eV) exhibited a good IC_{50} value compared to the standard drug Chloroquine, showing IC_{50} values of 0.042 μM and 0.054 μM , respectively. Lower chemical hardness (η)

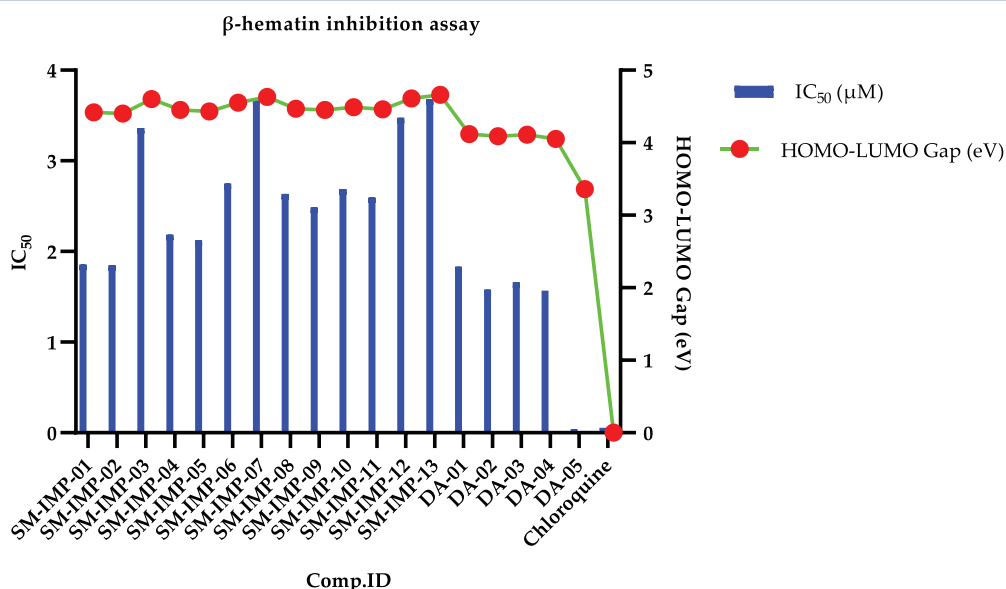


Fig. 11. (Color online) The results of the inhibition of β -hematin formation assay (IC_{50} values, μM) of tested compounds as (SM-IMP-01) to SM-IMP-13), and (DA-01-05), respectively. Wherein, Chloroquine was used as a standard antimalarial drug.

values of hydrazide series (DA-01-DA-05) with first two series (molecules, SM-IMP-01 to SM-IMP-13) explain higher bioactivity values of hydrazide series. In the literature, it was found that lower chemical hardness (η) values would likely have relation with strong bioactivity.^{14,15,31} Similarly, higher softness (S) values of SM-IMP-13 (S: 0.80 eV and 0.60 eV, respectively) and DA-05 within their respective series would likely have connection with their lower IC_{50} values. The cytotoxicity values calculated using 'BSL assay' are also following similar analogy as explained above. Considering our current data, we can say that hydrazide core with bromo-Imidazo[1,2-*a*]pyridine-3-carboxamides would serve as potential antimalarial agents in near future.

2.7. *In-silico* pharmacokinetic calculations

2.7.1. *The Physicochemical properties*

The Physicochemical properties of various compound are described in Table 4. Log-P denotes the compound's hydrophilicity; if a compound is hydrophilic, the value of Log-P is negative. Our data demonstrate that all of the derivatives have positive scores, indicating that they are all lipophilic. A greater Log-P value might result in inadequate solubility and absorption qualities. Number of hydrogen bond donors (nHA) and number of hydrogen bond acceptors (nHD) are also shown in Table 4 including electronic density (By using electronic density ρ , we can determine easily ground energy state and all other properties of molecules) and molecular weight. DA-01-DA05 series lies more in the optimal range as compared to SM-IMP-01 to SM-IMP-13 series, respectively.

2.7.2. *Boiled-egg model analyses of synthesized compounds*

It is well known that apart from efficacy and toxicity profiles of lead or drug-like candidates, many of assessed hits would fail at the stage of pharmacokinetics and bioavailability stages.²⁵ This is due to two main aspects of absorption of drug matters: (1) Gastrointestinal and (2) Brain accesses. The earlier estimations of ADME analyses (absorption, distribution, metabolism and excretion) actually decreased the number of failures of hit molecules at pharmacokinetics stages.²⁵ Nowadays, various machine learning-based models are available on handy which can predict such profiles within short span of time, although they may have false-positives or negatives,

Table 4. Physicochemical properties of the compounds.

| Structure code | Molecular weight | nHA | nHD | Electronic density | AlogP |
|----------------|------------------|-----|-----|--------------------|-------|
| SM-IMP-01 | 423.10 | 2 | 1 | 1.078 | 4.05 |
| SM-IMP-02 | 441.09 | 2 | 1 | 1.081 | 4.25 |
| SM-IMP-03 | 459.08 | 2 | 1 | 1.085 | 4.46 |
| SM-IMP-04 | 457.55 | 2 | 1 | 1.082 | 4.71 |
| SM-IMP-05 | 475.54 | 2 | 1 | 1.087 | 4.92 |
| SM-IMP-06 | 451.16 | 2 | 1 | 1.084 | 5.02 |
| SM-IMP-07 | 451.16 | 2 | 1 | 1.082 | 4.43 |
| SM-IMP-08 | 344.21 | 2 | 1 | 1.057 | 3.30 |
| SM-IMP-09 | 362.20 | 2 | 1 | 1.063 | 3.51 |
| SM-IMP-10 | 378.65 | 2 | 1 | 1.071 | 3.97 |
| SM-IMP-11 | 396.64 | 2 | 1 | 1.079 | 4.17 |
| SM-IMP-12 | 372.26 | 2 | 1 | 1.066 | 4.27 |
| SM-IMP-13 | 372.26 | 2 | 1 | 1.067 | 3.69 |
| DA-01 | 450.13 | 3 | 1 | 1.081 | 4.12 |
| DA-02 | 468.12 | 3 | 1 | 1.079 | 4.32 |
| DA-03 | 464.15 | 3 | 1 | 1.082 | 4.60 |
| DA-04 | 480.15 | 4 | 1 | 1.089 | 4.10 |
| DA-05 | 495.12 | 5 | 1 | 1.091 | 4.01 |

still increasing usage of same would definitely help researchers to narrow down the screening list of hit molecules, accelerating the drug discovery. One of such tools is 'SwissADME' (<http://www.swissadme.ch/index.php>).⁵² Thus, in order to check the plausible GI absorption profiles for our 18 imidazopyridines, we used 'Boiled-egg' model (The *Brain Or Intestinal EstimateD permeation* method). This model is based on the polarity indexes of molecules. From our boiled-egg model analyses, we noted that for series (SM-IMP-01 to SM-IMP-13), all molecules lie in 'yellow zone' of Blood-Brain Barrier (BBB) permeabilities; wherein among carbonylhydrazide, molecule, (DA-05) falls in 'white zone; indicating good GI absorption profile of same (Table 6). The overall analyses of all compounds suggested that these compounds have BBB penetrations and they need to be optimized further for better GI profiles in near future.

2.7.3. *Lipinski's rule calculations (Drug-likeness analysis)*

It is very evident that pharmacokinetic parameters play very critical roles in the developments of new

drugs from scratch obtained hits. Unfavorable ADMET factors ultimately result in drug candidature failures.⁵² Thus, in order to assess varieties of pharmacokinetics parameters, we subjected all synthesized compounds for 'QikProp' screening (Table 5). Except molecules DA-02, DA-03 and SM-IMP-05 all molecules showed no violations of Lipinski rule of five (Ro5: 5 H-bond donors (HBD), 10 H-bond acceptors (HBA), the molecular weight >500, and Clog *P* > 5), which is crucial while considering 'Drug likenesses'. Moreover, for rule of three (molecular weight <300, the cLogP ≤ 3, HBD ≤ 3 and HBA ≤ 3) violations, many compounds represented not more than 1 violation. Absorption is a process by which drug candidature reaches systemic circulation via different routes of drug administrations (such as oral and intravenous) and drugs are supposed to have sufficient permeabilities in order to cross lipophilic cell membranes, for example MDCK and Caco2 cells. QikProp analyses as represented in Table 5, showed that except compound (DA-05), all compounds displayed good

(100%) human oral absorption values compared to standard drugs Ciprofloxacin (48.777%) and Fluconazole (81.93%). From the analysis on 'QPPCaco', we have noted the fact that all compounds have very good Caco-2 cells permeabilities (as represented by higher values >1500 nm/s). Moreover, values for 'QplogPo/w' (Predicted octanol/water partition coefficient) were obtained within the said acceptable range of 'QikProp' (QplogPo/w < 6). Pertaining to distribution, this can be guided via PBP and BBB parameters (plasma binding protein and blood brain barrier, respectively). It is also known that drugs acting on central nervous system (CNS) have to cross BBB barrier. From our analyses on 'QplogBB' values, we noted that many of our synthesized molecules may cross BBB, which was adherent to the results obtained from 'Boiled-egg' model analysis, except (DA-05). Concerning metabolism, which is a process by which a drug molecule (xenobiotic) is transformed into more water-soluble metabolites facilitating excretion, mostly but not always via urine. Results exhibited that

Table 5. *In-silico* ADME analyses of synthesized compounds using QikProp*.

| Title | #Stars | Volume | QplogPo/w | QPlogHERG | QPPCaco | #metab | Percent human oral absorption | PSA | Rule of five | Rule of three |
|---------------|--------|----------|-----------|-----------|----------|--------|-------------------------------|---------|--------------|---------------|
| DA-01 | 1 | 1106.595 | 4.849 | -6.262 | 1939.616 | 2 | 100 | 62.148 | 0 | 1 |
| DA-02 | 1 | 1159.675 | 5.12 | -6.083 | 1938.691 | 3 | 100 | 62.153 | 1 | 1 |
| DA-03 | 2 | 1122.718 | 5.086 | -6.132 | 1940.541 | 2 | 100 | 62.14 | 1 | 1 |
| DA-04 | 1 | 1181.477 | 4.941 | -6.139 | 1939.027 | 3 | 100 | 70.44 | 0 | 1 |
| DA-05 | 0 | 1146.632 | 3.883 | -5.507 | 207.841 | 3 | 91.165 | 106.703 | 0 | 1 |
| SM-IMP-01 | 0 | 1002.284 | 4.323 | -5.476 | 3116.367 | 3 | 100 | 48.85 | 0 | 0 |
| SM-IMP-02 | 1 | 1018.564 | 4.559 | -5.361 | 3119.494 | 2 | 100 | 48.849 | 0 | 1 |
| SM-IMP-03 | 1 | 1037.066 | 4.801 | -5.336 | 3257.623 | 2 | 100 | 48.251 | 0 | 1 |
| SM-IMP-04 | 1 | 1046.441 | 4.816 | -5.405 | 3115.725 | 3 | 100 | 48.859 | 0 | 1 |
| SM-IMP-05 | 2 | 1061.138 | 5.018 | -5.303 | 3116.082 | 2 | 100 | 48.856 | 1 | 1 |
| SM-IMP-06 | 1 | 1101.623 | 4.844 | -5.208 | 3126.827 | 5 | 100 | 47.498 | 0 | 1 |
| SM-IMP-07 | 0 | 1105.184 | 4.989 | -5.443 | 3633.326 | 4 | 100 | 48.206 | 0 | 1 |
| SM-IMP-08 | 0 | 958.281 | 3.79 | -5.522 | 2711.177 | 3 | 100 | 49.385 | 0 | 0 |
| SM-IMP-09 | 0 | 974.224 | 4.024 | -5.403 | 2706.48 | 2 | 100 | 49.368 | 0 | 0 |
| SM-IMP-10 | 0 | 1001.803 | 4.278 | -5.444 | 2708.883 | 3 | 100 | 49.377 | 0 | 1 |
| SM-IMP-011 | 1 | 1015.261 | 4.475 | -5.332 | 2735.968 | 2 | 100 | 48.932 | 0 | 1 |
| SM-IMP-012 | 0 | 1057.396 | 4.307 | -5.248 | 2718.298 | 5 | 100 | 48.059 | 0 | 1 |
| SM-IMP-013 | 0 | 1060.633 | 4.453 | -5.472 | 3186.123 | 4 | 100 | 48.671 | 0 | 0 |
| Ciprofloxacin | 1 | 1015.58 | 0.28 | -3.246 | 13.434 | 0 | 48.777 | 97.988 | 0 | 1 |
| FLUCONAZOLE | 0 | 901.609 | 0.514 | -4.907 | 801.517 | 1 | 81.93 | 75.477 | 0 | 0 |

Notes. *#stars = Number of property or descriptor values that fall outside the 95% range of similar values for known drugs, QplogPo/w = Predicted octanol/water partition coefficient, QPPCaco = Predicted apparent Caco-2 cell permeability in nm/s, Percent Human Oral Absorption = Predicted human oral absorption on 0% to 100% scale, volume = Total solvent-accessible volume in cubic angstroms using a probe with a 1.4 Å radius, PSA = Van der Waals surface area of polar nitrogen and oxygen atoms, #metab = Number of likely metabolic reactions, dipole = Computed dipole moment of the molecule.

all synthesized compounds may undergo a minimum of 2 to a maximum of 5 numbers of metabolic reactions from Phase-I or/and Phase-II metabolic pathways. Finally for toxicity calculations, we used an online server 'admetSAR' (<http://lmmd.ecust.edu.cn/admetSAR2/>) and results depicted that many of our compounds would exhibit no mutagenicity or carcinogenesis. Considering cardiac toxicity via human ether-a-go-go related gene (hERG), we noted that our compounds have little higher but comparable 'QPlogHERG' values as of Ciprofloxacin (-3.246) and Fluconazole (-4.907).

2.8. Spectral data interpretations

Interpretations of spectral data for NMR, and FTIR are available in our previous publication. Spectra for $^1\text{H-NMR}$, $^{13}\text{C-NMR}$, mass of all compounds are available in *Supplementary Material (Supporting information, Figs. S7–S66)*.

2.9. 'SwissTargetPrediction' analyses

The probable predicted targets for synthesized compounds were accessed using the "SwissTargetPrediction" analyses.⁵³ Our analysis suggested that synthesized compounds had varied targets such as Kinases, Family of G-protein coupled receptors, Primary active transporters, Proteases and Voltage-gated ion channels. Their detailed reports are supplemented in Table S8.

3. MATERIALS AND METHODS

General Information

All chemicals and reagents used in this study were procured from Sigma Aldrich and Lab India, Pvt., Ltd., Mumbai. Further details on instruments and recording parameters are available in the *supporting information*.

3.1. Chemistry

Scheme 1 elaborates on the synthesis protocol adapted for molecules (SM-IMP-01) to (SM-IMP-13) as per previously published paper by our group.¹⁰ **Scheme 1** also details on hydrazides (DA-01- DA-05). Full details on synthesis have been attached in the *supporting information*.

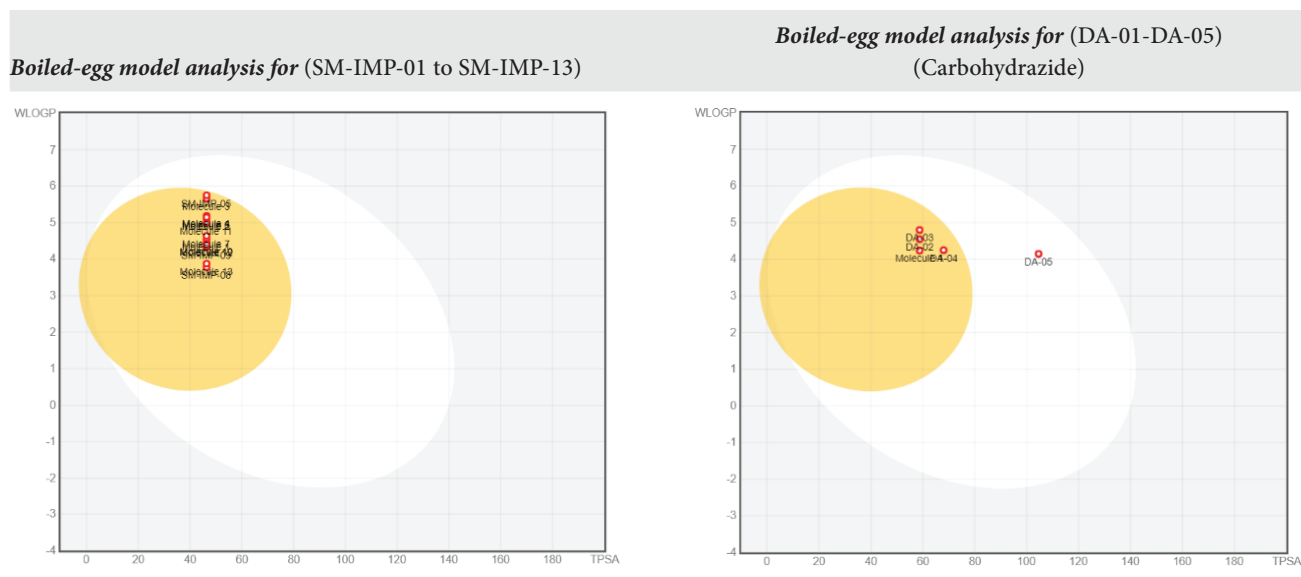
3.2. Bioactivity protocols

Bioactivity protocols such as BSL assay, *in vitro* anti-inflammatory assay, *in vitro* beta-haemitin assay, and antimicrobial analysis were performed as per literature-known protocols.⁴⁸ Their exact details have been provided in the *Supplementary Material*.

3.3. In-silico study protocol (Molecular Docking and MM/GBSA calculations)

For our study on synthesized Imidazopyridine analogues, we aimed to analyze their plausible binding

Table 6. Boiled-egg model analyses of all synthesized compounds (SM-IMP-01 to SM-IMP-13 and DA-01-05).



mechanisms using the molecular docking simulations with 'Glide, Schrodinger, LLC, NY, 2022' tool. Before proceeding for actual docking step, we downloaded required X-ray crystal structure of protein target of *Plasmodium*. We downloaded its 3D-crystal structure from the protein database bank (<http://www.rcsb.org>, the Research Collaboratory for Structural bioinformatics (RCSB)) with PDB code as 3BPF (Resolution: 2.90 Å; Falcipain-2 with its inhibitor, E64, which has key role in hemozoin pathway). The selection of this PDB id was based on the prior literature analysis. The downloaded crystal structure was then pre-processed, minimized and finally optimized using the 'protein preparation wizard' of Maestro 12.1 Platform, 2022.¹ Then, all 2D structures of ligands (Imidazopyridines) were first drawn using 'Chemdraw Ultra 12.0' and saved in '.sdf' format; which were then imported in Maestro platform and further processed for their energy minimizations steps using 'LigPrep, Schrodinger, LLC, NY, 2022' module. Ionization states and generation of numbers of conformers were set to defaults. Finally, grid was generated with radii of 20 Å into the receptor lattice (considering the locations of concerned internal ligands) and utilized for the molecular docking analysis using 'Glide/XP' (Extra Precision mode). Table 1, enlists best docked compounds and their docking scores with selected target under this study protocol. For proper 2D/3D-visualizations of ligand-protein interactions; we implemented 'BIOVIA Discovery studio visualizer version 19.1.0.18287 (Dassault systems, Paris, France)'. We also calculated Prime-MM/GBSA (molecular mechanics generalized born surface area (MM/GBSA)) energies for best docked complexes using 'Prime' module (Schrodinger LLC, NY, 2022).³¹

Formula expanded is given as follows:

$$\Delta G_{(\text{bind})} = \Delta G_{(\text{solv})} + \Delta E_{(\text{MM})} + \Delta G_{(\text{SA})},$$

where

- ΔG_{solv} is the difference in GBSA solvation energy of the 3BPF-inhibitor complex and the sum of the solvation energies for unliganded 3BPF and inhibitor.
- ΔE_{MM} is a difference in the minimized energies between 3BPF — inhibitor complex and the sum of the energies of the unliganded 3BPF and inhibitor.
- ΔG_{SA} is a difference in surface area energies of the complex and the sum of the surface area energies for the unliganded 3BPF and inhibitor.

Prime MM-GBSA calculates the energy of optimized free receptors, free ligand, and a complex of the ligand

with a receptor. It also calculates the ligand strain energy by placing ligand in a solution which was autogenerated by VSGB 2.0 suit. The prime energy visualizer presented the visualization of energy.

3.4. *In-Silico* BOILED-egg model and ADMET predictions

For all synthesized compounds, *in-silico* Gastrointestinal absorptions and BBB penetrations BBB accessibility have been determined using online web-server, 'SwissADME' (<http://www.swissadme.ch/index.php>). While ADME properties have been calculated using 'QikProp' module of Schrodinger, LLC, NY, 2022 drug discovery suite.

3.5. Density-functional theory

For our current set of compounds, we used the DFT methods and optimized ground states of imidazopyridines using the Gaussian 09 package. All the investigated structures were optimized by using the DFT calculations which use three-parameter Becke, Lee-Yang-Parr (B3-LYP) functional including the D3 correction for dispersion and the 6-311+G (*d*, *p*) basis sets. Optimized parameters related to the electronic properties were investigated including the geometric parameters, frontier molecular orbitals (FMO) and the global reactivity biological descriptors. The energy gap can be compared with some of the molecular properties such as reactivity and electrical conductivity and is defined as follows.

$$E_g = E_{\text{LUMO}} - E_{\text{HOMO}}, \quad (1)$$

where energy gap is denoted with E_g , energies of lowest unoccupied molecular orbital denoted as E_{LUMO} and energies of highest occupied molecular orbital denoted as E_{HOMO} , respectively. Other electronic properties also considered including the hardness (η), softness (*S*), chemical potential (μ) and electrophilicity index (ω) values were determined using the Koopman's theorem. The chemical stability and reactivity can be correlated with the chemical hardness (η), electronegativity (χ), softness (*S*) and electrophilicity index (ω).

Equations (1) and (2) were used to calculate the values of the ionization potential (IP) and electron affinity (EA):

$$\text{IP} = -E_{\text{HOMO}}, \quad (1)$$

$$\text{EA} = -E_{\text{LUMO}}. \quad (2)$$

For global hardness η and electronegativity χ values we used Eqs. (3) and (4):

$$\eta = \frac{[IP - EA]}{2} = \frac{[E_{LUMO} - E_{HOMO}]}{2}, \quad (3)$$

$$\chi = \frac{[IP + EA]}{2} = \frac{[E_{LUMO} + E_{HOMO}]}{2}. \quad (4)$$

And global electrophilicity ω value was calculated in the following equation:

$$\omega = \frac{\mu^2}{2\eta}, \quad (5)$$

where $\mu = \frac{E_{LUMO} + E_{HOMO}}{2}$ is the chemical potential of the system.

Finally, the global softness σ value was computed with the following equation:

$$\sigma = \frac{1}{2\eta}. \quad (6)$$

Moreover, we have also calculated **Mulliken charge distribution analysis**. For all calculations, gaussian09 suite, and for the visualization, Gauss View 6 (Dennington RD, Keith TA, Millam JM. GaussView, version 6.0. 16. Semichem Inc. Shawnee Mission KS. 2016.) utility were used.

3.6. Spectral data of synthesized compounds

The spectral data for all the synthesized compounds are available in the supporting information.

3.7 'SwissTargetPrediction' analyses for prediction of target classes

For all synthesized compounds, we evaluated their probable targets by using the online webserver 'SwissTargetPrediction' available at [<http://www.swisstargetprediction.ch/>].

4. CONCLUSION

In summary, a series of known 13 IMPCs (2,7-dimethylimidazo[1,2-*a*]pyridine-3-carboxamides) along with five carbohydrazide analogues were synthesized and characterized for their spectroscopic data. Synthesized analogues were found to have comparable antimalarial activity. The most significant

result was obtained for **SM-IMP-02**, and **DA-05**, which inhibited β -hematin formation significantly: IC_{50} : 1.849 and 0.042 μ M, respectively. Molecular docking results of **DA-05** on target 3bpf (Falcipain-2 with its inhibitor, E64) suggested that this compound was having highest MM/GBSA dg_{bind} energy of -55.91 KJ.mol⁻¹. This indicated that molecular target for (**DA-05**) might be on hemozoin pathway of *Plasmodium falciparum*. It was also found that, a compound (**DA-05**) had lower energy gap ($E_g = 3.36$ eV), which denotes that this compound might have the highest activity. By looking at BSL assay data, the same compound exhibited 10% mortality of nauplii at 1 μ g/ml, which was comparable with standard 5-FU. However, in order to arrive at exact conclusions, a 2D-QSAR study might be carried out in future. Furthermore, carbohydrazide (**DA-05**) demonstrated greater electronegativity and also the highest softness values. Our molecular modeling techniques used so far in this study suggested that the *in-silico* (molecular docking, binding free energy analysis and DFT calculations) results are actually supporting the observed experimental bioactivities of imidazopyridine analogues. Thus, we can also say that they are conforming to each other. Finally, our evaluation for *in-silico* ADMET pointed out the facts that several modifications must be required in order to reduce BBB accessibility, and to increase their water solubility. The proposed hit molecule, **DA-05** could also be used for in-detailed antimalarial potentials using higher *in vivo* models. Moreover, it can also be seen that compounds with 6,8-dibromo substituents would be prone to exhibit highest bioactivity, if they are not coupled with hydrazide moiety. However, we believe that our preliminary *in vitro* data may be useful for researchers to develop potent analogues of IMPCs in near future.

ACKNOWLEDGMENTS

Richie R. Bhandare would like to thank the Dean's office of College of Pharmacy and Health Sciences, Ajman University, UAE for their support. SM wish to thank Department of Pharmaceutical Sciences and Technology, BIT, Mesra, India. SM and AP also thanks for the provision of Schrodinger Small molecule drug discovery tool available at Department of Pharmaceutical Sciences & Technology, BIT, Mesra, India. The Author, Dr. Mozaniel Santana de Oliveira, thanks the Ministry of Science, Technology, and Innovation (MCTI)/National Council for Scientific and Technological Development (CNPq)/Institutional Training Program-(PCI), for the scholarship (process

number: 300983/2022-0). Oberdan Oliveira Ferreira and Suraj N. Mali with equal contribution in this paper.

FUNDING INFORMATION

Edital 02/2023 PAPQ/PROPESP-Universidade Federal do Pará, publication fee payment.

CONFLICTS OF INTEREST

The authors declare no conflict of interest.

ORCID

Suraj N. Mali  <https://orcid.org/0000-0003-1995-136X>

References

1. Kumar, P.; Kadyan, K.; Duhan, M.; Sindhu, J.; Singh, V.; Saharan, B. S. Design, Synthesis, Conformational and Molecular Docking Study of Some Novel Acyl Hydrazone Based Molecular Hybrids as Antimalarial and Antimicrobial Agents. *Chem. Cent. J.* **2017**, *11*, 1–14, doi:10.1186/s13065-017-0344-7.
2. World Health Organization, World Malaria Report 2022, 2022, <https://www.who.int/teams/global-malaria-programme/reports/world-malaria-report-2022>, Accessed 27 March 2023.
3. Towie, N. Malaria Breakthrough Raises Spectre of Drug Resistance. *Nature* **2006**, *440*, 852–854, doi:10.1038/440852b.
4. Tisnerat, C.; Dassonville-Klimpt, A.; Gosselet, F.; Sonnet, P. Antimalarial Drug Discovery: From Quinine to the Most Recent Promising Clinical Drug Candidates. *Curr. Med. Chem.* **2022**, *29*, 3326–3365, doi:10.2174/0929867328666210803152419.
5. Egan, T. J. Haemozoin Formation. *Mol. Biochem. Parasitol.* **2008**, *157*, 127–136, doi:10.1016/j.molbiopara.2007.11.005.
6. Samala, G.; Nallangi, R.; Devi, P. B.; Saxena, S.; Yadav, R.; Sridevi, J. P.; Yogeewari, P.; Sriram, D. Identification and Development of 2-methylimidazo [1, 2-a] Pyridine-3-carboxamides as *Mycobacterium tuberculosis* Pantothenate Synthetase Inhibitors. *Bioorg. Med. Chem.* **2014**, *22*, 4223–4232, doi:10.1016/j.bmc.2014.05.038.
7. Khetmalis, Y. M.; Chitti, S.; Wunnava, A. U.; Kumar, B. K.; Kumar, M. M. K.; Murugesan, S.; Sekhar, K. V. G. C. Design, Synthesis and Anti-mycobacterial Evaluation of Imidazo[1, 2-a]pyridine Analogues. *RSC Med. Chem.* **2022**, *13*, 327–342, doi:10.1039/D1MD00367D.
8. Samanta, S.; Kumar, S.; Aratikatla, E. K.; Ghorpade, S. R.; Singh, V. Recent Developments of Imidazo [1, 2-a] Pyridine Analogues as Antituberculosis Agents. *RSC Med. Chem.* **2023**, doi:10.1039/D3MD00019B.
9. Pulipati, L.; Sridevi, J. P.; Yogeewari, P.; Sriram, D.; Kantevari, S. Synthesis and Antitubercular Evaluation of Novel Dibenzo [b, d] Thiophene Tethered Imidazo [1, 2-a] Pyridine-3-Carboxamides. *Bioorganic Med. Chem. Lett.* **2016**, *26*, 3135–3140, doi:10.1016/j.bmcl.2016.04.088.
10. Jadhav, B.; Kenny, R.; Nivid, Y.; Mandewale, M.; Yamgar, R. Synthesis and Evaluation of Antituberculosis Activity of Substituted 2,7-Dimethylimidazo[1,2-a]Pyridine-3-Carboxamide Derivatives. *Open J. Med. Chem.* **2016**, *6*, 59–69, doi:10.4236/ojmc.2016.64006.
11. Jadhav, B. S.; Purohit, V. P.; Yamgar, R. S.; Kenny, R. S.; Mali, S. N.; Chaudhari, H. K.; Mandewale, M. C. Synthesis and In-silico Identification of New Bioactive 1, 3, 4-Oxadiazole Tagged 2, 3-Dihydroimidazo [1, 2-a]Pyridine Derivatives. *Curr. Bioact. Compd.* **2021**, *17*, 318–330, doi:10.2174/1573407216999200625222014.
12. Mali, S. N.; Pandey, A. Recent Developments in Medicinal and In Silico Applications of Imidazopyridine Derivatives: Special Emphasis on Malaria, Trypanosomiasis, and Tuberculosis. *Chem. Afr.* **2022**, *1*–22, doi:10.1007/s42250-022-00462-w.
13. Mali, S. N.; Anand, A.; Zaki, M. E. A.; Al-Hussain, S. A.; Jawarkar, R. D.; Pandey, A.; Kuznetsov, A. Theoretical and Anti-*Klebsiella pneumoniae* Evaluations of Substituted 2,7-dimethylimidazo[1,2-a]pyridine-3-carboxamide and Imidazopyridine Hydrazone Derivatives. *Molecules* **2023**, *28*, 2801, doi:10.3390/molecules28062801.
14. Mali, S. N.; Pandey, A. Molecular Modeling Studies on 2,4-Disubstituted Imidazopyridines as Anti-malarials: Atom-based 3D-QSAR, Molecular Docking, Virtual Screening, In-silico ADMET and Theoretical Analysis. *J. Comput. Biophys. Chem.* **2021**, *20*, 267–282, doi:10.1142/S2737416521500125.
15. Mali, S. N.; Pandey, A.; Thorat, B. R.; Lai, C. H. Multiple 3D- and 2D-Quantitative Structure–Activity Relationship Models (QSAR), Theoretical Study and Molecular Modeling to Identify Structural Requirements of Imidazopyridine Analogues as Anti-Infective Agents against Tuberculosis. *Struct. Chem.* **2022**, *33*, 679–694, doi:10.1007/s11224-022-01879-2.
16. Mishra, N. P.; Mohapatra, S.; Sahoo, C. R.; Raiguru, B. P.; Nayak, S.; Jena, S.; Padhy, R. N. Design, One-pot Synthesis, Molecular Docking Study, and Antibacterial

- Evaluation of Novel 2H-Chromene Based Imidazo [1, 2-a] Pyridine Derivatives as Potent Peptide Deformylase Inhibitors. *J. Mol. Struct.* **2021**, *1246*, 1–15, doi:10.1016/j.molstruc.2021.131183.
17. Althagafi, I.; Abdel-Latif, E. Synthesis and Antibacterial Activity of New Imidazo [1, 2-a] Pyridines Fused with Pyridine, Thiazole or Pyrazole Moiety. *Polycycl. Aromat. Compd.* **2021**, *42*, 4487–4500, doi:10.1080/10406638.2021.1894185.
18. Thakur, A.; Pereira, G.; Patel, C.; Chauhan, V.; Dhaked, R. K.; Sharma, A. Design, One-pot Green Synthesis and Antimicrobial Evaluation of Novel Imidazopyridine Bearing Pyran Bis-Heterocycles. *J. Mol. Struct.* **2020**, *1206*, 1–13, doi:10.1016/j.molstruc.2020.127686.
19. Ebenezer, O.; Awolade, P.; Koorbanally, N.; Singh, P. New Library of Pyrazole–imidazo [1, 2- α] Pyridine Molecular Conjugates: Synthesis, Antibacterial Activity and Molecular Docking Studies. *Chem. Biol. Drug Des.* **2020**, *95*, 162–173, doi:10.1111/cbdd.13632.
20. Salhi, L.; Achouche-Bouzroua, S.; Nechak, R.; Nedjar-Kolli, B.; Rabia, C.; Merazig, H.; Poulain-Martini, S.; Dunach, E. Synthesis of Functionalized Dihydroimidazo [1, 2-A] Pyridines and 4-Thiazolidinone Derivatives from Maleimide, as New Class of Antimicrobial Agents. *Synth. Commun.* **2020**, *50*, 412–422, doi:10.1080/00397911.2019.1699933.
21. Kuthyala, S.; Shankar, M. K.; Nagaraja, G. K. Synthesis, Single-Crystal X-Ray, Hirshfeld and Antimicrobial Evaluation of some New Imidazopyridine Nucleus Incorporated with Oxadiazole Scaffold. *ChemistrySelect* **2018**, *3*, 12894–12899, doi:10.1002/slct.201802011.
22. Devi, N.; Jana, A. K.; Singh, V. Assessment of Novel Pyrazolopyridinone Fused Imidazopyridines as Potential Antimicrobial Agents. *Karbala Int. J. Mod. Sci.* **2018**, *4*, 164–170, doi:10.1016/j.kijoms.2018.01.003.
23. Al-Tel, T. H.; Al-Qawasmeh, R. A.; Zaarour, R. Design, Synthesis and In Vitro Antimicrobial Evaluation of Novel Imidazo [1, 2-a] Pyridine and Imidazo [2, 1-b] [1, 3] Benzothiazole Motifs. *Eur. J. Med. Chem.* **2011**, *46*, 1874–1881, doi:10.1016/j.ejmech.2011.02.051.
24. Starr, J. T.; Sciotti, R. J.; Hanna, D. L.; Huband, M. D.; Mullins, L. M.; Cai, H.; Gage, J. W.; Lockard, M.; Rauckhorst, M. R.; Owen, R. M. 5-(2-Pyrimidinyl)-imidazo [1, 2-a] Pyridines are Antibacterial Agents Targeting the ATPase Domains of DNA Gyrase and Topoisomerase IV. *Bioorganic Med. Chem. Lett.* **2009**, *19*, 5302–5306, doi:10.1016/j.bmcl.2009.07.141.
25. Mali, S. N.; Pandey, A. Synthesis of New Hydrazones using a Biodegradable Catalyst, their Biological Evaluations and Molecular Modeling Studies (Part-II). *J. Comput. Biophys. Chem.* **2022**, *21*, 857–882, doi:10.1142/S2737416522500387.
26. Thorat, B. R.; Rani, D.; Yamgar, R. S.; Mali, S. N. Synthesis, Spectroscopic, In-vitro and Computational Analysis of Hydrazones as Potential Antituberculosis Agents: (Part-I). *Comb. Chem. High Throughput Screen.* **2020**, *23*, 392–401, doi:10.2174/1386207323999200325125858.
27. Mali, S. N.; Thorat, B. R.; Gupta, D. R.; Pandey, A. Mini-Review of the Importance of Hydrazides and their Derivatives — Synthesis and Biological Activity. *Eng. Proc.* **2021**, *11*, 21, doi:10.3390/ASEC2021-11157.
28. Mali, S. N.; Pandey, A.; Thorat, B. R.; Lai, C.-H. Greener Synthesis, In-Silico and Theoretical Analysis of Hydrazides as Potential Antituberculosis Agents (Part 1). *Chem. Proc.* **2022**, *8*, 86, doi:10.3390/ecsoc-25-11655.
29. Ragavendran, J. V.; Sriram, D.; Patel, S. K.; Reddy, I. V.; Bharathwajan, N.; Stables, J.; Yogeewari, P. Design and Synthesis of Anticonvulsants from a Combined Phthalimide–GABA–anilide and Hydrazone Pharmacophore. *Eur. J. Med. Chem.* **2007**, *42*, 146–151, doi:10.1016/j.ejmech.2006.08.010.
30. Damghani, T. *et al.*, Imidazopyridine Hydrazone Derivatives Exert Antiproliferative Effect on Lung and Pancreatic Cancer Cells and Potentially Inhibit Receptor Tyrosine Kinases Including c-Met. *Sci. Rep.* **2021**, *11*, 3644, doi:10.1038/s41598-021-83069-4.
31. Mishra, V. R.; Ghanavatkar, C. W.; Mali, S. N.; Qureshi, S. I.; Chaudhari, H. K.; Sekar, N. Design, Synthesis, Antimicrobial Activity and Computational Studies of Novel Azo Linked Substituted Benzimidazole, Benzoxazole and Benzothiazole Derivatives. *Comput. Biol. Chem.* **2019**, *78*, 330–337, doi:10.1016/j.compbiolchem.2019.01.003.
32. Mali, S. N.; Pandey, A. Multiple QSAR and Molecular Modelling for Identification of Potent Human Adenovirus Inhibitors. *J. Indian Chem. Soc.* **2021**, *98*, 100082, doi:10.1016/j.jics.2021.100082.
33. Kapale, S. S.; Mali, S. N.; Chaudhari, H. K. Molecular Modelling Studies for 4-oxo-1,4-dihydroquinoline-3-carboxamide Derivatives as Anticancer Agents. *Med. Drug Discov.* **2019**, *2*, 100008, doi:10.1016/j.medidd.2019.100008.
34. Chakraborty, A.; Pan, S.; Chattaraj, P. Biological Activity and Toxicity: A Conceptual DFT Approach, in *Applications of Density Functional Theory to Biological and Bioinorganic Chemistry*, Vol. 150, 2013, pp. 143–180.
35. Frisch, M. *et al.* (eds.) *Gaussian 16, Revision B.01* (Gaussian, Wallingford, CT, 2016).

36. McLean, A. D.; Chandler, G. Contracted Gaussian-Basis Sets for Molecular Calculations. I. Second Row Atoms, $Z = 11-18$. *J. Chem. Phys.* **1980**, *72*, 5639–5648, doi:10.1063/1.438980.
37. Mabkhot, Y. N.; Aldawsari, F. D.; Al-Showiman, S. S.; Barakat, A.; Soliman, S. M.; Choudhary, M. I.; Yousuf, S.; Mubarak, M. Novel Enaminone Derived from Thieno[2,3-b]thiene: Synthesis, X-ray Crystal Structure, HOMO, LUMO, NBO Analyses and Biological Activity. *Chem. Cent. J.* **2015**, *9*, 24, doi:10.1186/s13065-015-0100-9.
38. Kumar, S.; Saini, V.; Maurya, I. K.; Sindhu, J.; Kumari, M.; Kataria, R.; Kumar, V. Design, Synthesis, DFT, Docking Studies and ADME Prediction of Some New Coumarinyl Linked Pyrazolylthiazoles: Potential Standalone or Adjuvant Antimicrobial Agents. *PLoS One* **2018**, *13*, e0196016, doi:10.1371/journal.pone.0196016.
39. Waghulde, S.; Kale, M. K.; Patil, V. Brine Shrimp Lethality Assay of the Aqueous and Ethanolic Extracts of the Selected Species of Medicinal Plants. *Proceedings* **2019**, *41*, 47, doi:10.3390/ecsoc-23-06703.
40. Moshi, M. J.; Innocent, E.; Magadula, J. J.; Otieno, D. F.; Weisheit, A.; Mbabazi, P. K.; Nondo, R. S. O. Brine Shrimp Toxicity of Some Plants used as Traditional Medicines in Kagera Region, North Western Tanzania. *Tanzan. J. Health Res.* **2010**, *12*, 63–67, doi:10.4314/thrb.v12i1.56287.
41. Matata, D. Z.; Moshi, M. J.; Machumi, F.; Ngassapa, O. D.; Swanepoel, B.; Oosthuizen, K.; Venables, L.; Koekemoer, T.; Heydenreich, M.; Kazyoba, P. E.; van de Venter, M. Isolation of a New Cytotoxic Compound, 3-((Z)-heptadec-14-enyl) Benzene-1-ol from *Rhus Natalensis* Root Extract. *Phytochem. Lett.* **2020**, *36*, 120–126, doi:10.1016/j.phytol.2020.01.024.
42. Arumugam, D. G.; Sivaji, S.; Dhandapani, K. V.; Nookala, S.; Ranganathan, B. Panchagavya Mediated Copper Nanoparticles Synthesis, Characterization and Evaluating Cytotoxicity in Brine Shrimp. *Biocatal. Agric. Biotechnol.* **2019**, *19*, 101132, doi:10.1016/j.bcab.2019.101132.
43. Apu, A. S.; Muhit, M. A.; Tareq, S. M.; Pathan, A. H.; Jamaluddin, A. T. M.; Ahmed, M. Antimicrobial Activity and Brine Shrimp Lethality Bioassay of the Leaves Extract of *Dillenia indica* Linn. *J. Young Pharm.* **2010**, *2*, 50–53, doi:10.4103/0975-1483.62213.
44. Chandra, S.; Chatterjee, P.; Dey, P.; Bhattacharya, S. Evaluation of In Vitro Anti-inflammatory Activity of Coffee against the Denaturation of Protein. *Asian Pac. J. Trop. Biomed.* **2012**, *2*, S178–S180, doi:10.1016/S2221-1691(12)60154-3.
45. Banerjee, M.; Kumar, H.; Sahu, S.; Das, A.; Parasar, P. Synthesis and In-vitro Protein Denaturation Screening of Novel Substituted Isoxazole/pyrazole Derivatives. *Rasayan J. Chem.* **2011**, *4*, 413–417.
46. Gondkar, A. S.; Deshmukh, V. K.; Chaudhari, S. R. Synthesis, Characterization and In-vitro Anti-inflammatory Activity of Some Substituted 1, 2, 3, 4 Tetrahydropyrimidine Derivatives. *Drug Invent. Today* **2013**, *5*, 175–181, doi:10.1016/j.dit.2013.04.004.
47. Wang, X. M.; Xin, M. H.; Xu, J.; Kang, B. R.; Li, Y.; Lu, S. M.; Zhang, S. Q. Synthesis and Antitumor Activities Evaluation of m-(4-morpholinoquinazolin-2-yl) Benzamides in Vitro and in Vivo. *Eur. J. Med. Chem.* **2015**, *96*, 382–395, doi:10.1016/j.ejmech.2015.04.037.
48. Mali, S. N.; Pandey, A. Synthesis, Computational Analysis, Antimicrobial, Antioxidant, Trypan Blue Exclusion Assay, β -hematin Assay and Anti-inflammatory Studies of Some Hydrazones (Part-I). *Curr. Comput. Aided Drug Des.* **2022**, doi:10.2174/1573409918666220929145824.
49. Mojarrab, M.; Shiravand, A.; Delazar, A.; Heshmati Afshar, F. Evaluation of in Vitro Antimalarial Activity of Different Extracts of *Artemisia aucheri* Boiss. and *A. armeniaca* Lam. and Fractions of the Most Potent Extracts. *Sci. World J.* **2014**, doi:10.1155/2014/825370.
50. Matsa, R.; Makam, P.; Kaushik, M.; Hoti, S. L.; Kannan, T. Thiosemicarbazone Derivatives: Design, Synthesis and In Vitro Antimalarial Activity Studies. *Eur. J. Pharm. Sci.* **2019**, *137*, 104986, doi:10.1016/j.ejps.2019.104986.
51. Agbektas, T.; Zontul, C.; Ozturk, A.; Huseynzada, A.; Ganbarova, R.; Hasanova, U.; Cinar, G.; Tas, A.; Kaya, S.; Chtita, S.; Silig, Y. Effect of azomethine group containing compounds on gene profiles in WNT and MAPK signal patterns in lung cancer cell line: In silico and in vitro analyses. *J. Mol. Struct.* **2023**, *1275*, 134619.
52. Daina, A.; Michielin, O.; Zoete, V. SwissADME: A Free Web Tool to Evaluate Pharmacokinetics, Drug-likeness and Medicinal Chemistry Friendliness of Small Molecules. *Sci. Rep.* **2017**, *7*, 42717, doi:10.1038/srep42717.
53. Gfeller, D.; Grosdidier, A.; Wirth, M.; Daina, A.; Michielin, O.; Zoete, V. SwissTargetPrediction: A Web Server for Target Prediction of Bioactive Small Molecules. *Nucleic Acids Res.* **2014**, *42* (W1), W32–W38, doi:10.1093/nar/gku293.